

April 2006

Structural effects on exchange in nanocluster perpendicular recording media

J. Zhou

University of Nebraska - Lincoln

Ralph Skomski

University of Nebraska-Lincoln, rskomski2@unl.edu

David J. Sellmyer

University of Nebraska-Lincoln, dsellmyer@unl.edu

Follow this and additional works at: <http://digitalcommons.unl.edu/physicsellmyer>

 Part of the [Physics Commons](#)

Zhou, J.; Skomski, Ralph; and Sellmyer, David J., "Structural effects on exchange in nanocluster perpendicular recording media" (2006). *David Sellmyer Publications*. 4.

<http://digitalcommons.unl.edu/physicsellmyer/4>

This Article is brought to you for free and open access by the Research Papers in Physics and Astronomy at DigitalCommons@University of Nebraska - Lincoln. It has been accepted for inclusion in David Sellmyer Publications by an authorized administrator of DigitalCommons@University of Nebraska - Lincoln.

Structural effects on exchange in nanocluster perpendicular recording media^{a)}

J. Zhou,^{b)} R. Skomski, and D. J. Sellmyer

*Department of Physics and Astronomy and Center for Materials Research and Analysis,
University of Nebraska, Lincoln, Nebraska 68588*

(Presented on 1 November 2005; published online 16 May 2006)

Nanostructured FePt:*M* (*M*=C,Ag,Cu) perpendicular magnetic recording media are investigated by numerical simulations and model calculations. Both intra- and intergranular exchanges are considered, and it is assumed that the interaction through the matrix is mediated by conduction electrons. Several limits, including free-electron-like Ruderman-Kittel-Kasuya-Yosida interactions, are considered. The atomic modeling yields effective intergranular coupling strengths that depend on both cluster radius and distance, on the magnetic properties of the clusters, and on the electronic nature of the medium. In the simulations, the exchange is approximated by a thin shell with reduced exchange and zero anisotropy. The simulations show that intergranular exchange reduces the coercivity of the system, and the magnetization reversal proceeds in a regime between localized nucleation and discrete domain-wall pinning, depending on the intergranular exchange. Coercivity and loop-shape reduction also depend on the geometry of the particle system. © 2006 American Institute of Physics. [DOI: 10.1063/1.2177423]

High-anisotropy nanocluster films are of great interest for extremely high-density recording, because they promise thermal stability with small grain size and low noise.¹⁻³ The large uniaxial anisotropy constant K_u of FePt and CoPt is the basis for creating coercivity H_c in $L1_0$ -based magnetic recording media. Examples are perpendicularly oriented nanoparticles of FePt embedded in nonmagnetic matrix, which have a grain size of 6 nm and are reported as promising candidates for future high-density recording.^{4,5}

For a single nanoparticle of FePt, the Stoner-Wohlfarth model predicts a coercivity of more than 100 kOe, and dilute FePt:C nanoclusters show that well-isolated particles behave in accordance with the Stoner-Wohlfarth model.⁶ However, in the (001) textured granular FePt:*M* thin films (*M*=C,Ag,Cu), there is a significant reduction of the coercivity because of the real structure of the films. For (001) textured FePt:*M*, a typical coercivity is about 20 kOe while the anisotropy field is about 60 kOe.^{4,5} There are two main reasons for the reduced coercivity: intragranular imperfections and intergranular interactions, including domain-wall pinning effects. In developing high-density recording media, it is important to understand these effects and their influence on the hysteretic behavior. Previous efforts towards understanding the reduction of the coercivity include various core-shell models for a single particle.^{7,8} For cluster sizes smaller than about 10 nm, the domain-wall jump is reminiscent of a Stoner-Wohlfarth rotation of individual grains.^{7,9} In magnetic recording media, the large anisotropy of $L1_0$ particles helps to ensure the thermal stability of the stored information. The coupling to a softer grain-boundary phase reduces the coercivity to facilitate writing, and it has been argued that this does not necessarily deteriorates the zero-field thermal stability of the medium.¹⁰ However, little attention has been

paid to the effect of intergranular exchange, which plays an important role in coupling the grains to determine the reversal mechanism.

When the nanograins are well separated by matrix with weak or no exchange interaction, the reversal is of the nucleation type, and individual grains rotate coherently. When the exchange within the matrix becomes stronger, the reversal mechanism changes to discrete domain-wall pinning, where nonequilibrium interaction domains are separated by pseudo-domain walls located between the clusters. In this regime, the reversal can be interpreted as a sequence of single-grain jumps.

In this paper, we investigate the effect of intergranular exchange on the magnetization reversal. We start with an analysis of intergranular exchange and then simulate the according hysteresis loops.

The effective exchange between two grains shows a complicated dependence on factors such as grain separation and size,¹¹ interface structure,¹² and matrix composition. Aside from atomic factors, the effective exchange is modified and generally reduced by micromagnetic effects. For example, in the limit of vanishing grain separation, an anti-

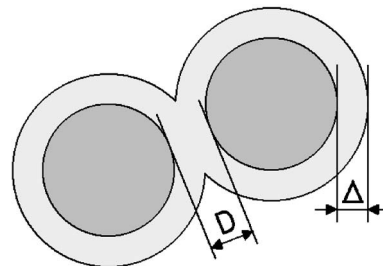


FIG. 1. Geometry of the core-shell model used in the simulations. The effective exchange decreases monotonously with increasing surface-to-surface distance D and reaches zero at $D=2\Delta$.

^{a)}No proof corrections received from author prior to publication.

^{b)}Electronic mail: jzhou@unlserve.unl.edu

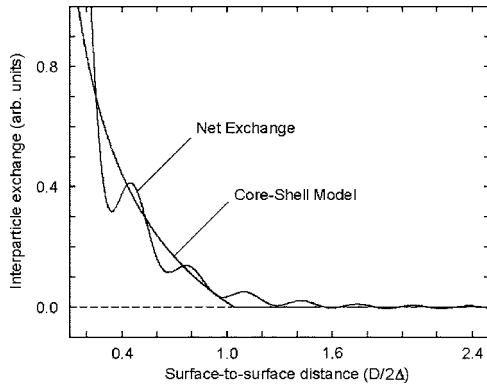


FIG. 2. Schematic distance dependence of the intergranular exchange between two spherical particles in a matrix. The true net exchange involves both decaying and oscillatory contributions, depending on the matrix material.

parallel moment orientation is punished by a huge exchange energy, and the magnetization gradient is forced to penetrate deep into the grains.¹³

The influence of the grain size is seen as a dependence on the surface curvature.¹⁴ It is conceivable, for example, that the intergranular exchange is dominated by parallel surfaces separated by a few interatomic layers of a simple metal. Then the effective exchange may be approximated by the two-dimensional Ruderman-Kittel-Kasuya-Yosida (RKKY) interaction,

$$J(D) \sim \sin(2k_F D)/D^2, \quad (1)$$

where D is the surface-to-surface distance. For curved surfaces that nearly touch each other, $J(D)$ must be integrated over the surface, $J_{\text{eff}} = \int J[D_{\text{loc}}(x, y)] dx dy$. For spherical particles of radii R_I and R_{II} ,

$$D_{\text{loc}} = D + \frac{1}{2} \left(\frac{1}{R_I} + \frac{1}{R_{II}} \right) (x^2 + y^2). \quad (2)$$

For the RKKY interactions between grains that nearly touch each other, the integration over $D_{\text{loc}}(x, y)$ yields

$$J_{\text{eff}}(D) \sim \left(\frac{R_I R_{II}}{R_I + R_{II}} \right) \text{Ci}(2k_F D), \quad (3)$$

where the integral cosine $\text{Ci}(x) = \text{const.} + \ln(x) + O(x^2)$. In other words, the RKKY model predicts a weak (logarithmic) divergence of J_{eff} for very small interparticle distances.

In reality, the free-electron type RKKY model must be replaced by more elaborate interactions, and the resulting $J_{\text{eff}}(D)$ contains various oscillatory and monotonically decaying contributions. Typically, these contributions are negligibly small for interparticle distances larger than about 1 nm. In the following, we approximate the interparticle exchange by an interaction shell with finite thickness Δ and reduced interatomic exchange. Figure 1 shows the geometry of the shell model used to fit the oscillatory behavior of Fig. 2 and Eq. (3). Aside from averaging over the oscillations, the model yields a sharp cutoff at $D=2\Delta$, because the shells must overlap to realize nonzero intergranular exchange. Figure 2 compares the predictions of the shell-interaction model with a typical oscillatory exchange. The core-shell model is then used to perform the numerical calculations.

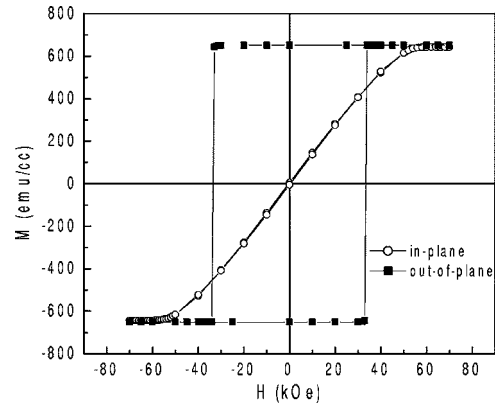


FIG. 3. Typical simulated hysteresis loops of an eight-particle system. The particles are (001) oriented and randomly distributed. The size ranging is from 4 to 8 nm with a 0.7–1 nm thick shell.

To analyze the effects of geometry of the recording media on coercivity and hysteresis-loop shape, we use the OOMMF code provided by NIST.¹⁵ The simulations are based on the Landau-Lifshitz-Gilbert equation. A few structural parameters, including particle size, position randomness, and the exchange stiffness, are varied. In the Stoner-Wohlfarth model, the parallel and perpendicular hysteresis loops reach $M=M_s$ at the same field H_A . In reality, both intersection fields are reduced, but the reduction of the coercivity is more pronounced.^{4,5}

Our model consists of eight uniaxial FePt particles with diameters ranging from 3 to 8 nm, randomly distributed in nonmagnetic matrix in a region of $14 \times 14 \times 9 \text{ nm}^3$. The easy axis of these particles is along [001] direction, motivated by the (001) texture of the modeled experimental system. The particles have a core-shell magnetic structure with a soft-shell thickness of about 0.8 nm. The volume fraction of FePt particles in the matrix is about 60%–70%. This is above the percolation threshold, and neighboring particles are likely to touch each other, or be connected by exchange. The respective anisotropy, exchange, and magnetization parameters are $K_u = 4 \times 10^7 \text{ erg/cc}$, $A = 1 \times 10^{-6} \text{ erg/cm}$, and $M_s = 1000 \text{ emu/cc}$ for the cores, and $K_u = 0$, $A = 0.5 - 0.8 \times 10^{-6} \text{ erg/cm}$, $M_s = 500 \text{ emu/cc}$ for the shells. The numerical cell size is chosen as 0.5 nm.

Figure 3 shows typical simulated hysteresis loops with the field parallel and normal to the easy axis. The coercivity and the anisotropy field are both smaller than the theoretical value $H_A = 2K_u/M_s$, due to the reduced anisotropy of the shell region. The simulated coercivity H_c is 33 kOe while anisotropy field H_A is 54 kOe. The coercivity is reduced disproportionately. Figure 4 shows simulated spin structure change of the system simulation 4 (see Table I) under small field-changing pace at coercive field. The nanoparticles with diameters of 4–8 nm sizes percolate through the shell phase forming grain boundaries between the particles. The z direction is perpendicular to the plane, and the field is applied along $-z$ direction ([001]). White areas represent nonmagnetic regions. In the magnetic regions, the magnetization is characterized by the area darkness. Light area has upward moment and dark area has downward moment. The reversal starts from the smaller particles, as shown in Fig. 4(a). The

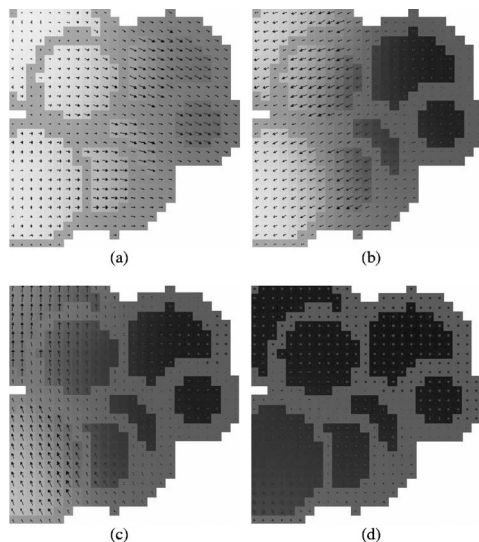


FIG. 4. A Simulated magnetization reversal in the nanoparticles (simulation 4 in Table I), with the magnitude of the magnetic field increasing from (a) to (d). The field is along the $-z$ direction, i.e., into the plane. The magnetization changes from $+z$ (light area) to $-z$ (dark area). The small arrows are neglectable x - y components. The intermediate exchange in the shell ($A=0.8 \times 10^{-6}$ erg/cm) shifts the reversal mechanism into the transition regime from localized nucleation to discrete pinning.

spin structures show that incoherent nucleation controls the reversal throughout the percolated particles. For the intermediate exchange stiffness of boundary/shell ($A=0.8 \times 10^{-6}$ erg/cm), this reversal is in the regime between localized nucleation and discrete pinning.⁹

Table I shows the simulation results for different parameters. Comparison of the results reveals the effects of size, exchange, and geometry. The size distribution has a far-reaching influence on the coercivity, because smaller particles have a lower coercivity and the intergranular exchange promotes the propagation of the reversal mode from small to big grains. Note, in this context, that the system with an average particle size of 6 nm has a coercivity larger than that of the 5.5 nm system (simulation 3 vs 1).

The effective exchange stiffness of the shell is also a factor affecting the coercivity. A strong exchange in the shell reduces the coercivity when the reversal mechanism changes towards the regime of discrete pinning. This result is in agreement to our previous observations in a similar granular Sm-Co/Cu-Ti system.⁹

The comparison of isolated particles (simulation 5, realized by reducing the randomness of particles position) with contacting particles (simulation 4) shows the effect of geom-

TABLE I. Simulated coercivities for different geometries and parameters.

Simulation No.	Size (nm)	Shell thickness (nm)	A (shell, 10^{-6} erg/cm)	H_c (kOe)
1	3–7	0.7–1	0.5	32
2 ^a	3–7	0.7–1	0.5	42
3	4–8	0.7–1	0.5	42
4	4–8	0.7–1	0.8	33
5 ^b	6	0.8	0.8	46

^aLess particle contact.

^bSingle particle.

etry and packing fraction. Granular films show smaller coercivities than the single core-shell sphere, and less particle contact (simulation 2) yield higher coercivities than the more particle-contact system (simulation 1).

Typically, for strong intergranular exchange, the magnetization reversal proceeds by discrete domain-wall pinning. In this regime, the reversal can be interpreted as a sequence of single-grain jumps. For cluster sizes smaller than about 10 nm, the domain-wall jump is reminiscent of a Stoner-Wohlfarth rotation of individual grains. Bigger clusters exhibit a complicated incoherent intragranular reversal that is only marginally affected by intergranular exchange. However, when the clusters nearly touch each other, the reversal mechanism change to a complicated cooperative mode and the consideration of individual clusters is no longer meaningful. In the hysteresis loop, this is seen as a cooperative enhancement of the slope dM/dH at H_c and which would be accompanied by an increase of media noise. The onset of the cooperative behavior is at a particle separation of somewhat less than 1 nm, depending on particle geometry and matrix materials. Details will be discussed elsewhere. The reversal process shown in Fig. 4 is close to this transition region.

In summary, we have performed the analytical and numerical calculations to investigate the magnetization reversal in anisotropic nanostructured FePt: M recording media. The interaction through the matrix is approximated by a thin shell with reduced interatomic exchange. Analyzing the exchange interactions yields an effective intergranular coupling that depend on both cluster radius and distance, on the magnetic properties of the clusters or particles, and on the electronic nature of the medium. The reversal mechanism depends on both intra- and intergranular features. Magnetization reversal in moderately coupled granular magnets is controlled by localized nucleation, and both inter- and intragranular exchanges yield a coercivity reduction.

This research is supported by NSF-MRSEC, INSIC, the W. M. Keck Foundation, and CMRA.

¹X. W. Wu, K. Y. Guslienko, R. W. Chantrell, and D. Weller, Appl. Phys. Lett. **82**, 3475 (2003).

²D. J. Sellmyer, M. L. Yan, Y. F. Xu, and R. Skomski, IEEE Trans. Magn. **41**, 560 (2005).

³S. Kang, Z. Jia, S. Shi, D. E. Nikles, and J. W. Harrell, Appl. Phys. Lett. **86**, 062503 (2005).

⁴M. L. Yan, X. Z. Li, L. Gao, S. H. Liou, D. J. Sellmyer, R. J. M. van de Veerdonk, and K. W. Wierman, Appl. Phys. Lett. **83**, 3332 (2003).

⁵C. P. Luo, S. H. Liou, L. Gao, Y. Liu, and D. J. Sellmyer, Appl. Phys. Lett. **77**, 2225 (2000).

⁶Y. F. Xu, M. L. Yan, J. Zhou, and D. J. Sellmyer, J. Appl. Phys. **97**, 10J320 (2005).

⁷J. Zhou, R. Skomski, K. D. Sorge, and D. J. Sellmyer, Scr. Mater. **53**, 453 (2005).

⁸W. Scholz, D. Suess, T. Schrefl, and J. Fidler, J. Appl. Phys. **95**, 6807 (2004).

⁹J. Zhou, A. Kashyap, Y. Liu, R. Skomski, and D. J. Sellmyer, IEEE Trans. Magn. **40**, 2940 (2004).

¹⁰R. H. Victora and S. Xiao, IEEE Trans. Magn. **41**, 537 (2005).

¹¹R. Skomski, A. Kashyap, Y. Qiang, and D. J. Sellmyer, J. Appl. Phys. **93**, 6477 (2003).

¹²Y. Qiang, R. F. Sabirianov, S. S. Jaswal, H. Haberland, and D. J. Sellmyer, Phys. Rev. B **66**, 064404 (2002).

¹³R. Skomski, J. Phys.: Condens. Matter **15**, R841 (2003).

¹⁴R. Skomski, J. Magn. Mater. **272–276**, 1476 (2004).

¹⁵<http://math.nist.gov/oommf>